Reaction Pathways and Energy Barriers for Alkaline Hydrolysis of Carboxylic Acid Esters in Water Studied by a Hybrid Supermolecule-Polarizable Continuum Approach

Chang-Guo Zhan,*,† Donald W. Landry,† and Rick L. Ornstein*,‡

Contribution from the Department of Medicine, College of Physicians & Surgeons, Columbia University, New York, New York 10032, and the Pacific Northwest National Laboratory, Battelle-Northwest, Environmental Technology Division, Mailstop K2-21, Richland, Washington 99352

Received October 22, 1999

Abstract: Reaction pathways, solvent effects, and energy barriers have been determined for the base-catalyzed hydrolysis of two representative alkyl esters in aqueous solution, using a hybrid supermolecule-polarizable continuum approach. Four solvent water molecules were explicitly included in the supermolecular reaction coordinate calculations; the remaining solvent water was modeled as a polarizable dielectric continuum surrounding the supermolecular reaction system. Two competing reaction pathways were observed, sharing a common first step, i.e. the formation of the tetrahedral intermediate. One pathway involves a direct proton transfer in the second step, i.e. the decomposition of the tetrahedral intermediate. A second pathway involves a water-assisted proton transfer during the decomposition of the tetrahedral intermediate. The direct participation of the solvent water molecule in the proton-transfer process significantly drops the energy barrier for the decomposition of the tetrahedral intermediate. Thus, the energy barrier calculated for the decomposition of the tetrahedral intermediate through the water-assisted proton transfer becomes lower than the barrier for the formation of the tetrahedral intermediate, while that through the direct proton transfer is higher. The computations reveal the important effect of solvent hydrogen bonding on energy barriers; without explicit consideration of the hydrogen-bonding effects, the calculated energy barriers for the formation of the tetrahedral intermediate become ∼4−5 kcal/mol smaller. The favorable pathway involving water-assisted proton transfer and the energy barriers calculated using the hybrid supermolecule-polarizable continuum approach, including both the hydrogen-bonding effects and the remaining bulk solvent effects, are consistent with available experimental results. The energy barriers calculated for the first step of the hydrolysis in aqueous solution are in excellent agreement with the reported experimental data for methyl acetate and methyl formate.

Introduction

The hydrolysis of carboxylic acid esters is one of the most fundamental and thoroughly studied chemical reactions in chemistry and biochemistry.[1−3] A great many experimental and theoretical studies[4−16] on ester hydrolysis have been carried out, resulting in a rich array of possible reaction mechanisms. We will focus only on the most common mechanism involving specific base-catalyzed hydrolysis, *i.e.* hydroxide ion-catalyzed hydrolysis.[3c] Besides extensive interests within chemistry, the mechanism of the base-catalyzed hydrolysis of esters figures prominently in many biological processes[3d,17] such as the metabolism of the neurotransmitter acetylcholine and the degradation of cocaine. Understanding the mechanism of base-

† Columbia University.

‡ Pacific Northwest National Laboratory.

(1) (a) Bender, M. L. *Chem. Rev.* **1960**, *60*, 53. (b) Johnson, S. L. *Adv. Phys. Org. Chem.* **1967**, *5*, 237. (c) Jencks, W. P. *Chem. Rev.* **1972**, *72*, 705.

(2) (a) Bamford, C. H.; Tipper, C. F. H. Eds. *Ester Formation and Hydrolysis*; Elsevier: Amsterdam, 1972; Vol. 10. (b) Ingold, C. K. *Structure and Mechanism in Organic Chemistry*, 2nd ed.; Cornell University Press: Ithaca, New York, 1969; p 1131.

(3) (a) Jones, R. A. Y. *Physical and Mechanistic Organic Chemistry*; Cambridge University Press: Cambridge, 1979; p 227. (b) McMurry, J. *Organic Chemistry*, 2nd ed.; Cole Publishing: California, 1988. (c) Lowry, T. H.; Richardson, K. S. *Mechanism and Theory in Organic Chemistry*, 3rd ed.; Harper and Row: New York, 1987. (d) Williams, A. In *Enzyme Mechanisms*; Page, M. I., Williams, A., Eds.; Burlington: London, 1987; p 123.

(4) (a) Polanyi, M.; Szabo, A. L. *Trans. Faraday Soc.* **1934**, *30*, 508. (b) Bender, M. L.; Dewey, R. S. *J. Am. Chem. Soc.* **1956**, *78*, 317. (c) Samuel, D.; Silver, B. L. *Adv. Phys. Org. Chem.* **1965**, *3*, 123.

(5) (a) Bender, M. L.; Heck, H. d'A. *J. Am. Chem. Soc.* **1967**, *89*, 1211. (b) Shain, S. A.; Kirsch, J. F. *J. Am. Chem. Soc.* **1968**, *90*, 5848. (c) Rylander, P. N.; Tarbell, D. S. *J. Am. Chem. Soc.* **1950**, *72*, 3021. (d) Fukuda, E. K.; McIver, R. T., Jr. *J. Am. Chem. Soc.* **1979**, *101*, 2498.

(6) (a) Faigle, J. F. G.; Isolani, P. C.; Riveros, J. M. *J. Am. Chem. Soc.* **1976**, *98*, 2049. (b) Takashima, K.; Riveros, J. M. *J. Am. Chem. Soc.* **1978**, *100*, 6128. (c) Johlman, C. L.; Wilkins C. L. *J. Am. Chem. Soc.* **1985**, *107*, 327.

(7) Takashima, K.; Jose, S. M.; do Amaral, A. T. *J. Chem. Soc., Chem. Commun.* **1983**, 1255.

(8) (a) Bender, M. L.; Thomas, R. J. *J. Am. Chem. Soc.* **1961**, *83*, 4189. (b). Bender, M. L.; Matsui, H.; Thomas, R. J.; Tobey, S. W. *J. Am. Chem. Soc.* **1961**, *83*, 4193. (c) Bender, M. L.; Heck, H., d'A. *Ibid.* **1967**, *89*, 1211. (d) Bender, M. L.; Ginger, R. D.; Unik, J. P. *Ibid.* **1958**, *80*, 1044. (e) O'Leary, M. H.; Marlier, J. F. *J. Am. Chem. Soc.* **1979**, *101*, 3300. (f) Guthrie, J. P. *J. Am. Chem. Soc.* **1991**, *113*, 3941. (h) Hengge, A. *J. Am. Chem. Soc.* **1992**, *114*, 6575. (h) Marlier, J. F. *J. Am. Chem. Soc.* **1993**, *115*, 5953.

(9) (a) Bunnett, J. F. *J. Am. Chem. Soc.* **1961**, *83*, 4978. (b) Rogers, G. A.; Bruice, T. C. *J. Am. Chem. Soc.* **1973**, *95*, 4452; **1974**, *96*, 2473; **1974**, *96*, 2481. (c) Gravitz, N.; Jencks, W. P. *J. Am. Chem. Soc.* **1974**, *96*, 489. (c) Capon, B.; Ghosh, K.; Grieve, D. M. A. *Acc. Chem. Res.* **1981**, *14*, 306. (d) McClelland, R. A.; Santry, L. J. *Acc. Chem. Res.* **1983**, *16*, 394.

(10) (a) Bowden, K. *Adv. Phys. Org. Chem.* **1993**, *28*, 171. (b) Bowden, K. *Chem. Soc. Rev.* **1995**, *25*, 431. (c) Bowden, K.; Byrne, J. M. *J. Chem. Soc., Perkin Trans. 2* **1996**, 2203; **1997**, 123. (d) Bowden, K.; Izadi, J.; Powell, S. L. *J. Chem. Rev.* **1997**, 404. (e) Bowden, K.; Battah, S. *J. Chem. Soc., Perkin Trans. 2* **1998**, 1603. (f) Li, P.; Zhao, K.; Deng, S.; Landry, D. W. *Helv. Chim. Acta* **1999**, *82*, 85.

catalyzed hydrolysis, in particular the transition state, led to the design of stable analogues that could inhibit acetylcholinesterase[18] and elicit monoclonal antibodies capable of catalyzing the hydrolysis of the cocaine.[19] A deeper understanding of ester hydrolysis mechanisms should provide additional insights into numerous biological and chemical processes.

The base-catalyzed hydrolysis of the majority of common alkyl esters occurs by the attack of hydroxide ion at the carbonyl carbon.[3c] This mode of hydrolysis has been designated as $B_{AC}2$ (base-catalyzed, acyl-oxygen cleavage, bimolecular),[3c] and is believed to occur by a two-step mechanism.[3] However, a concerted pathway can arise in the case of esters containing very good leaving groups (corresponding to a low pK_a value for R′OH).[8] The generally accepted two-step mechanism consists of the formation of a tetrahedral intermediate (first step), followed by decomposition of the tetrahedral intermediate to products $RCOO^-$ + R′OH (second step).[3c] According to reported experimental heavy-atom kinetic isotope effects on alkaline hydrolysis, the first step is usually rate-determining for the hydrolysis of alkyl esters in solution.[3c,8h] On the other hand, the second step is believed to be rate-determining in the gas phase.[16] The dramatic difference between the reactions in gas phase and in solution has been attributed to the strong solvation of the hydroxide ion in solution.[11,13,20]

Reaction pathways for the base-catalyzed hydrolysis of alkyl esters have also been studied theoretically in gas phase.[16] Concerning the solvent effects on the energy barrier for the ester hydrolysis, Sherer, Turner, and Shields *et al.*[13] carried out semiempirical molecular orbital calculations on the first step, i.e. the formation of the tetrahedral intermediate. Employing Cramer and Truhlar's SM3 continuum solvation model[21] together with the PM3 molecular orbital method, they evaluated the energy barrier for the first step of the base-catalyzed hydrolysis of methyl acetate in aqueous solution as 19.8 kcal/

mol, compared with the experimental activation energy, 10.45 kcal/mol[22] (pure water) or 12.2 kcal/mol[23] (62% acetone in water), for the whole hydrolysis process. After all of the calculations in the present study were finished and the manuscript was ready for submission, another related study was recently reported by Haeffner et al.[24] They attempted to examine the catalytic effect of water in the base-catalyzed hydrolysis of methyl acetate at the MP2/6-31+G(d)//HF/6-31+G(d) level of theory. They explicitly accounted for two solvent water molecules in the reaction pathway calculations on the second step of the $B_{AC}2$ process and employed the polarizable continuum model (PCM)[25] to evaluate the bulk solvent effects. According to their reported results, the first step of the $B_{AC}2$ process in aqueous solution should always be rate-determining no matter whether the second step is assisted directly by a solvent water molecule or not. However, their transition-state structure for the first step was simply determined by a partial optimization with the constraint of the distance between the carbonyl carbon and the hydroxide oxygen, while the geometries of others species were fully optimized. Thus, the relative magnitudes of the energy barriers for the first and second steps still remain to be compared, and the role of solvent water has not been fully elucidated. A more complete, theoretical study of the solvent effects on the energy barriers for the base-catalyzed hydrolysis of alkyl esters based on first-principle quantum chemical calculations would advance the understanding of hydrolysis mechanisms in aqueous solution.

We attempt herein to examine the solvent effects on the energy barriers for the base-catalyzed hydrolysis of alkyl esters and explore the role of solvent water in the hydrolysis process, taking methyl acetate and methyl formate as representative alkyl esters. A series of first-principle calculations were carried out based on the hybrid supermolecule-polarizable continuum approach in which a few solvent water molecules are explicitly included in the supermolecular reaction coordinate calculations and the remainder are modeled as a polarizable dielectric continuum surrounding the supermolecular reaction system. The calculations are compared with the available experimental results.

Calculation Methods

Pure self-consistent reaction field (SCRF) calculations based on dielectric continuum models[26] completely ignore the solvent structure and, therefore, might not account for some important effects caused by specific solute−solvent interactions, especially for chemical reactions assisted directly by solvent molecules. The pure reaction field calculation can be improved by coupling with a supermolecule model that includes solute and a few solvent molecules interacting with the solute. The hybrid supermolecule-polarizable continuum approach used in this study was based on a supermolecule model in which four solvent water molecules having hydrogen bonds with solutes are explicitly included in the reaction system. Geometries of the transition states, reactants, and intermediates for the supermolecular reaction system were first fully optimized by employing density functional theory (DFT) using

(11) (a) Dewar, M. J. S.; Storch, D. M. *J. Chem. Soc., Chem. Commun.* **1985**, *94*. (b) Dewar, M. J. S.; Storch, D. M. *J. Chem. Soc., Perkin Trans. 2* **1989**, 877.

(12) (a) Hori, K. *J. Chem. Soc., Perkin Trans. 2* **1992**, 1629. (b) Hori, K.; Kamimura, A.; Kimoto, J.; Gotoh, S.; Ihara, Y. *J. Chem. Soc., Perkin Trans. 2* **1994**, 2053. (c) Hori, K.; Kamimura, A.; Ando, K.; Nakao, Y.; Mizumura, M. *Tetrahedron* **1994**, *53*, 2053.

(13) (a) Sherer, E. C.; Turner, G. M.; Shields, G. C. *Int. J. Quantum Chem. Quantum Biol. Symp.* **1995**, *22*, 83. (b) Turner, G. M.; Sherer, E. C.; Shields, G. C. *Int. J. Quantum Chem. Quantum Biol. Symp* **1995**, *22*, 103.

(14) (a) Sherer, E. C.; Turner, G. M.; Lively, T. N.; Landry, D. W.; Shields, G. C. *J. Mol. Model.* **1996**, *2*, 62. (b) Sherer, E. C.; Yang, G.; Turner, G. M.; Shields, G. C.; Landry, D. W. *J. Phys. Chem. A* **1997**, *101*, 8526.

(15) (a) Williams, I. H.; Spangler, D.; Femec, D. A.; Maggiora, G. M.; Schowen, R. L. *J. Am. Chem. Soc.* **1980**, *102*, 6621. (b) Williams, I. H.; Maggiora, G. M.; Schowen, R. L. *J. Am. Chem. Soc.* **1980**, *102*, 7831. (c) Williams, I. H.; Spangler, D.; Femec, D. A.; Maggiora, G. M.; Schowen, R. L. *J. Am. Chem. Soc.* **1983**, *105*, 31.

(16) Zhan, C.-G.; Landry, D. W.; Ornstein, R. L. *J. Am. Chem. Soc.* **2000**, *122*, 1522.

(17) (a) Fersht, A. *Enzyme Structure and Mechanism*; Freeman: San Francisco, 1977. (b) Jencks, W. P. *Catalysis in Chemistry and Enzymology*; Dover Publications: New York, 1987.

(18) Ecobichon, D. J. In *Casarett & Doull's Toxicology*, 5th ed.; Klaassen, C. D., Ed.; McGraw-Hill: New York, 1996; pp 643.

(19) (a) Landry D. W.; Zhao, K.; Yang, G. X.-Q.; Glickman, M.; Georgiadis, T. M. *Science* **1993**, *259*, 1899. (b) Yang, G.; Chun, J.; Arakawa-Uramoto, H.; Wang, X.; Gawinowicz, M. A.; Zhao, K.; Landry, D. W. *J. Am. Chem. Soc.* **1996**, *118*, 5881. (c) Mets, B.; Winger, G.; Cabrera, C.; Seo, S.; Jamdar, S.; Yang, G.; Zhao, K.; Briscoe, R. J.; Almonte, R.; Woods, J. H.; Landry, D. W. *Proc. Natl. Acad. Sci. U.S.A.* **1998**, *95*, 10176.

(20) (a) Weiner, S. J.; Singh, U. C.; Kollman, P. A. *J. Am. Chem. Soc.* **1985**, *107*, 2219. (b) Madura, J. D.; Jorgensen, W. L. *J. Am. Chem. Soc.* **1986**, *108*, 2517. (c) Lipez, X.; Dejaegere, A.; Karplus, M. *J. Am. Chem. Soc.* **1999**, *121*, 5548. (d) Bakowies, D.; Kollman, P. A. *J. Am. Chem. Soc.* **1999**, *121*, 5712.

(21) Cramer, C. J.; Truhlar, D. G. *J. Comput. Chem.* **1992**, *13*, 1089.

(22) Fairclough, R. A.; Hinshelwood, C. N. *J. Chem. Soc.* **1937**, 538.

(23) Rylander, P. N.; Tarbell, D. S. *J. Am. Chem. Soc.* **1950**, *72*, 3021.

(24) Haeffner, F.; Hu, C.-H.; Brinck, T.; Norin, T. *J. Mol. Struct. (THEOCHEM)* **1999**, *459*, 85.

(25) (a) Miertus, S.; Scrocco, E.; Tomasi, J. *Chem. Phys.* **1981**, *55*, 117. (b) Miertus, S.; Tomasi, J. *Chem. Phys.* **1982**, *65*, 239. (c) Cossi, M.; Barone, V.; Cammi, R.; Tomasi, J. *Chem. Phys. Lett.* **1996**, *255*, 327.

(26) (a) Tomasi, J.; Persico, M. *Chem. Rev.* **1994**, *94*, 2027. (b) Cramer, C. J.; Truhlar, D. G. In *Solvent Effects and Chemical Reactions*; Tapia, O., Bertran, J., Eds.; Kluwer: Dordrecht, 1996; p 1. (c) Cramer, C. J.; Truhlar, D. G. *Chem. Rev.* **1999**, *99*, 2161. (d) Chipman, D. M. *J. Chem. Phys.* **1997**, *106*, 10194. (e) Chipman, D. M. *J. Chem. Phys.* **1999**, *110*, 8012.

Hydrolysis of Carboxylic Acid Esters in Water

J. Am. Chem. Soc., Vol. 122, No. 11, 2000 2623

the B3LYP functional[27] with the 6-31G(d) basis set, and were then refined at the B3LYP/6-31++G(d,p) level of theory. Vibrational frequency calculations were carried out to confirm the transition states and stable structures optimized, and intrinsic reaction coordinate (IRC) calculations[28] were performed to verify the expected connections of the first-order saddle points with the local minima found on the potential energy surface. Zero-point vibration energy (ZPVE) corrections to the total energy were carried out based on the frequency calculations at the B3LYP/6-31G(d) level. Geometries optimized at the B3LYP/6-31++G(d,p) level were employed for energy evaluation using second-order Møller−Plesset (MP2) theory with basis sets 6-31++G(d,p), 6-311++G(d,p), 6-311++G(2d,2p), and 6-311++G(3d,2p). Numerical results obtained for the base-catalyzed hydrolysis of methyl acetate in the gas phase[16] indicate that the MP2/6-31++G(d,p)//MP2/6-31++G-(d,p) results are basically the same as the corresponding MP2/6-31++G(d,p)//B3LYP/6-31++G(d,p) results and that energy calculations at the MP2/6-31++G(d,p) level of theory are adequate for studying the energy profile of the hydrolysis. Replacing the MP2 method with the QCISD(T) method, while holding constant the basis set, did not change the results significantly. For the energy barriers, the largest difference between the MP2/6-31++G(d,p)//B3LYP/6-31++G(d,p) and the MP2/6-31++G(d,p) results was 0.2 kcal/mol, and the largest difference between the MP2/6-31++G(d,p)//B3LYP/6-31++G(d,p) and the QCISD(T)/6-31++G(d,p)//MP2/6-31++G(d,p) results was 0.3 kcal/mol.[16] Unless indicated otherwise, the Gaussian94[29] and Gaussian98[30] programs were used to obtain the present results.

Finally, the remaining bulk solvent effects on the energy barriers were accounted for by performing self-consistent reaction field (SCRF) energy calculations on the supermolecules by using the geometries optimized at the B3LYP/6-31++G(d,p) level. For comparison, additional pure SCRF calculations were also carried out on the reaction system which does not explicitly include any solvent molecule by using the geometries optimized at the B3LYP/6-31++G(d,p) level. The SCRF method employed in this study was developed and implemented recently in the GAMESS program[31] by one of us (together with Bentley and Chipman),[32a] and may be called the fully polarizable continuum model (FPCM)[33] because both surface and volume polarization effects are fully determined in the SCRF calculation. Since the solute cavity surface is defined as a solute electron charge isodensity contour determined self-consistently during the FPCM iteration process,[32] the FPCM results, converged to the exact solution of the Poisson's equation with a given numerical tolerance, depend only on the value of the contour for a given dielectric constant under a particular quantum chemical calculation level.[32a,e] This single parameter value has been calibrated as 0.001 au.[32b] Thus, the 0.001 au contour was used for all the FPCM calculations

in this study. Regarding the quantum chemical calculation level used in the present FPCM calculations, previous continuum solvation calculations[32b] with the FPCM method indicate that solvent shifts of the energy change from one structure to another are not sensitive to the employed basis set when the volume polarization is included in the SCRF calculations, even if the energy change calculated in gas phase is very sensitive to the basis set. Furthermore, electron correlation effects on the solvent shifts calculated by the FPCM method are also not important.[32c] This issue was further examined in the present study by performing the pure SCRF calculations on the reaction system which does not explicitly include any solvent molecule at both the HF/6-31++G(d,p) and MP2/6-31++G(d,p) levels.[32d] Since the results calculated at the HF/6-31++G(d,p) level are almost identical to those calculated at the MP2/6-31++G(d,p) level (vide infra), we elected to perform the FPCM calculations on the supermolecules at the HF/6-31++G(d,p) level.

All the computations in this work were performed on Silicon Graphics, Inc. Origin 200 multiprocessor computers.

Results and Discussion

Geometries of Supermolecular Transition States, Intermediates, and Reactants. The important geometries optimized at the B3LYP/6-31++G(d,p) level for the hydrolysis of methyl acetate are depicted in Figure 1. Note that throughout this paper the suffix "a" refers to methyl acetate and "b" refers to methyl formate. All of the geometries optimized for methyl formate (not shown) are very similar to the corresponding geometries for methyl acetate. There is no difference between the qualitative results obtained for the hydrolysis of the two esters. Therefore, we may focus simply on methyl acetate in the following discussion of the reaction pathway.

As depicted in Figure 1, for the separated reactants, three solvent water molecules simultaneously form strong hydrogen bonds with the hydroxide oxygen, and the fourth water molecule forms a weaker hydrogen bond with the carbonyl oxygen of methyl acetate. The solvated hydroxide anion, HO⁻(H₂O)₃, attacks the carbonyl carbon of the solvated methyl acetate, CH₃-COOCH₃(H₂O), to form the tetrahedral intermediate INTa-(H₂O)₄ via the first transition state TS1a(H₂O)₄. During the process of this first reaction step, while the hydroxide oxygen gradually approaches the carbonyl carbon, two of the three water molecules having hydrogen bonds with the hydroxide gradually form new hydrogen bonds with the carbonyl oxygen and ester oxygen, respectively. While the new hydrogen bonds gradually form, the old hydrogen bonds of the two water molecules with the hydroxide gradually break. The intermediate INTa(H₂O)₄ is formed when the formation of the two new hydrogen bonds

(27) (a) Becke, A. D. *J. Chem. Phys.* **1993**, *98*, 5648. (b) Lee, C.; Yang, W.; Parr, R. G. *Phys. Rev. B* **1988**, *37*, 785.

(28) (a) Gonzalez, C.; Schlegel, H. B. *J. Chem. Phys.* **1989**, *90*, 2154. (b) Gonzalez, C.; Schlegel, H. B. *J. Phys. Chem.* **1990**, *94*, 5523.

(29) Frisch, M. J.; Trucks, G. W.; Schlegel, H. B.; Gill, P. M. W.; B. G. Johnson, B. G.; Robb, M. A.; Cheeseman, J. R.; Keith, T.; Petersson, G. A.; Montgomery, J. A.; Raghavachari, K.; Al-Laham, M. A.; Zakrzewski, V. G.; Ortiz, J. V.; Foresman, J. B.; Cioslowski, J.; Stefanov, B. B.; Nanayakkara, A.; Challacombe, M.; Peng, C. Y.; Ayala, P. Y.; Chen, W.; Wong, M. W.; Andres, J. L.; Replogle, E. S.; Gomperts, R.; Martin, R. L.; Fox, D. J.; Binkley, J. S.; Defrees, D. J.; Baker, J.; Stewart, J. P.; Head-Gordon, M.; Gonzalez, C.; Pople, J. A. *Gaussian 94*, Revision D.1; Gaussian, Inc.: Pittsburgh, PA, 1995.

(30) Frisch, M. J.; Trucks, G. W.; Schlegel, H. B.; Scuseria, G. E.; Robb, M. A.; Cheeseman, J. R.; Zakrzewski, V. G.; Montgomery, J. A.; Stratmann, R. E.; Burant, J. C.; Dapprich, S.; Millam, J. M.; Daniels, A. D.; Kudin, K. N.; Strain, M. C.; Farkas, O.; Tomasi, J.; Barone, V.; Cossi, M.; Cammi, R.; Mennucci, B.; Pomelli, C.; Adamo, C.; Clifford, S.; Ochterski, J.; Petersson, G. A.; Ayala, P. Y.; Cui, Q.; Morokuma, K.; Malick, D. K.; Rabuck, A. D.; Raghavachari, K.; Foresman, J. B.; Cioslowski, J.; Ortiz, J. V.; Stefanov, B. B.; Liu, G.; Liashenko, A.; Piskorz, P.; Komaromi, I.; Gomperts, R.; Martin, R. L.; Fox, D. J.; Keith, T.; Al-Laham, M. A.; Peng, C. Y.; Nanayakkara, A.; Gonzalez, C.; Challacombe, M.; Gill, P. M. W.; Johnson, B.; Chen, W.; Wong, M. W.; Andres, J. L.; Gonzalez, A. C.; Head-Gordon, M.; Replogle, E. S.; Pople, J. A. *Gaussian 98*, Revision A.6; Gaussian, Inc.: Pittsburgh, PA, 1998.

(31) Schmidt, M. W.; Baldridge, K. K.; Boatz, J. A.; Elbert, S. T.; Gordon, M. S.; Jensen, J. H.; Koseki, S.; Matsunaga, N.; Nguyen, K. A.; Su, S. J.; Windus, T. L.; Dupuis, M.; Montgomery, J. A. *J. Comput. Chem.* **1993**, *14*, 1347.

(32) (a) Zhan, C.-G.; Bentley, J.; Chipman, D. M. *J. Chem. Phys.* **1998**, *108*, 177. (b) Zhan, C.-G.; Chipman, D. M. *J. Chem. Phys.* **1998**, *109*, 10543. (c) Zhan, C.-G.; Chipman, D. M. *J. Chem. Phys.* **1999**, *110*, 1611. (d) For the FPCM calculations with MP2 method, the MP2 perturbation procedure was performed for electron correlation correction after the converged HF wave function of solute in reaction field is obtained. (e) Regarding the detail of the FPCM computation on a given solute under a given quantum mechanical approximation level, once the solute cavity is defined and the dielectric constant is known, the accuracy of the FPCM numerical computation depends only on the number of surface nodes (N) representing the cavity surface and number of layers (M) describing the volume polarization charge distribution within a certain, sufficiently large three-dimensional space outside the solute cavity. If one could use an infinite number of nodes and an infinite number of layers, then the numerical results obtained from the FPCM computation would be exactly the same as those determined by the exact solution of the Poisson's equation for describing the solvent polarization potential. We have shown that the accuracy of the FPCM numerical computations employed in this study with $N = 590$ and $M = 40$ (for a step of 0.3 Å) are higher than what required for listing Tables 1 and 2 in this paper. The dielectric constant of water used for the FPCM calculations is 78.5.

(33) Zhan, C.-G.; Norberto de Souza, O.; Rittenhouse, R.; Ornstein, R. L. *J. Am. Chem. Soc.* **1999**, *121*, 7279.
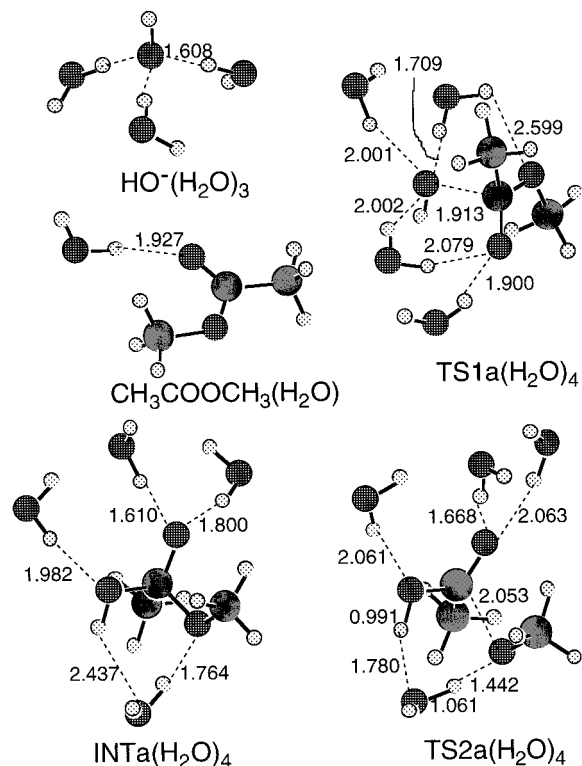
Figure 1. Geometries of the supermolecular transition states TS1a-$(H_2O)_4$ and TS2a$(H_2O)_4$, tetrahedral intermediate INTa$(H_2O)_4$, and reactants $HO^-(H_2O)_3$ and $CH_3COOCH_3(H_2O)$ optimized at the B3LYP/6-31++G(d,p) level for the hydrolysis of methyl acetate. The internuclear distances are given in Å.

Figure 2. Geometry of the supermolecular transition state TS2′a$(H_2O)_4$ associated with the direct proton transfer optimized at the B3LYP/6-31++G(d,p) level for the hydrolysis of methyl acetate. The internuclear distances are given in Å.

is complete, while the two old hydrogen bonds with the hydroxide are broken. Thus, in the structure of intermediate INTa$(H_2O)_4$ only one water molecule hydrogen-bonds to the hydroxide/hydroxyl oxygen, the second water molecule hydrogen-bonds to the ester oxygen, and the other two water molecules hydrogen-bond to the carbonyl oxygen. Thus, each of the three solute oxygen atoms in INTa$(H_2O)_4$ has a total of three chemical bonds, i.e. covalent and hydrogen bonds. The hydrogen-bond transfer is reflected in the transition-state structure TS1a$(H_2O)_4$, in which one of the water molecules has weaker hydrogen bonds with the hydroxide oxygen and carbonyl oxygen, simultaneously. Except for the hydrogen bonding to water, there is little difference between the first step of the hydrolysis for the supermolecular reaction system and the first step of the hydrolysis in water-free gas phase. Ignoring the solvent water molecules, the geometries of TS1a$(H_2O)_4$ and INTa$(H_2O)_4$ depicted in Figure 1 are very similar to the geometries of the first transition state (denoted by TS1a) and the tetrahedral intermediate (denoted by INTa) optimized for the hydrolysis of methyl acetate in gas phase.[16] We may conclude that the solvation within our consideration does not change the reaction pathway for the first step of the hydrolysis because no solvent molecule is directly involved in the change of covalent bonds.

However, a different story was found for the second step of the hydrolysis, i.e. the decomposition of the tetrahedral intermediate to products methanol and acetate. The decomposition of the tetrahedral intermediate requires a proton transfer from the hydroxide/hydroxyl oxygen to the ester oxygen, while the C−O bond between carbonyl carbon and ester oxygen gradually breaks. The IRC calculations starting from the second transition state TS2a$(H_2O)_4$ depicted in Figure 1 in two directions confirm that TS2a$(H_2O)_4$ connects with the intermediate INTa$(H_2O)_4$ and the expected products. It is notable that, for the reaction
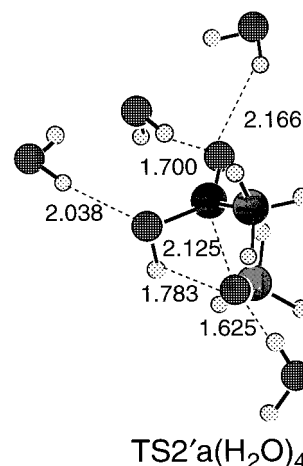
pathway associated with the transition state TS2a$(H_2O)_4$, the proton transfer from the hydroxide/hydroxyl oxygen to the ester oxygen is assisted by a solvent water molecule. The water molecule hydrogen-bonding with the ester oxygen in INTa-$(H_2O)_4$ structure gradually transfers a proton to the ester oxygen through the hydrogen bond, while the hydroxide/hydroxyl proton gradually transfers to the water oxygen. This indirect proton-transfer associated with the transition state TS2a$(H_2O)_4$ found for the supermolecular reaction system is different from the direct proton-transfer found for the reaction of methyl acetate with hydroxide ion in gas phase. To further understand the role of the water molecule assisting the proton transfer, we also found another transition state, TS2′a$(H_2O)_4$ depicted in Figure 2, associated with the pathway of the direct proton transfer for the supermolecular reaction system. Ignoring the four solvent water molecules, the TS2′a$(H_2O)_4$ structure depicted in Figure 2 is very similar to the structure of the second transition state (denoted by TS2a) for the hydrolysis of methyl acetate in gas phase.[16] Thus, two competing reaction pathways were found for the supermolecular reaction system. The two pathways share a common first step. The difference in energy barriers between the two reaction pathways will be discussed after discussion of the results obtained from the pure SCRF calculations.

Pure SCRF Calculations. The energy barriers obtained from the pure SCRF calculations for the two steps of the $B_{AC}2$ route of hydrolysis of methyl acetate and methyl formate are summarized in Table 1. The total energy of the separated reactants, RCOOR′ and HO^-, in gas phase is ∼15 kcal/mol higher than the first transition state for methyl acetate (TS1a), and is ∼13 kcal/mol higher than the first transition state for methyl formate (TS1b). For each of the methyl esters in gas phase, between the separated reactants and the first transition state (TS1), there is a hydrogen-bonded reactant complex (denoted by HBR)[16] whose energy is lower than both that of the transition state TS1 and the separated reactants. However, in aqueous solution the SCRF calculations gave the same qualitative result, that the separated reactants are more stable than both TS1 and HBR, while HBR is still more stable than TS1. It follows that in aqueous solution the HBR structure is not stable and that the reaction goes directly from the separated reactants to TS1. This is because the interaction between solvent water and the separated reactants is stronger than that between methyl acetate and hydroxide anion. Hence, the hydrogen-bonded complexes are not considered in Table 1.

Table 1. Energy Barriers (in kcal/mol) Calculated for the Base-Catalyzed Hydrolysis of Methyl Esters in Aqueous Solution by Performing Pure Self-Consistent Reaction Field Calculations with the 6-31++G(d,p) Basis Set[a]

	$CH_3COOCH_3 + HO^-$		$HCOOCH_3 + HO^-$	
	Ra → TS1a	INTa → TS2a	Rb → TS1b	INTb → TS2b
ΔE (gas phase, MP2)	-14.6^d	6.9	-13.1^e	6.2
ΔE (FPCM)[b]	7.3	10.3	5.3	11.0
ΔE (FPCM-MP2)[c]	7.2	10.5	5.2	11.2

[a] All calculations used geometries optimized at the B3LYP/6-31++G(d,p) level in gas phase. Ra and Rb represents the separated reactants $CH_3COOCH_3 + HO^-$ and $HCOOCH_3 + HO^-$, respectively. INT is the tetrahedral intermediate. TS1 and TS2 are the first and second transition states of the hydrolysis via the $B_{AC}2$ route, respectively. The ZPVE corrections were made for all of the values listed. [b] The energy barrier is taken as the sum of the ΔE (gas phase, MP2) value and the corresponding solvent shift determined by the FPCM calculations at the HF/6-31++G(d,p) level. [c] The FPCM calculations were also performed at the MP2/6-31++G(d,p) level. [d] The energy barrier calculated in gas phase is 1.1 kcal/mol which is the energy change from a hydrogen-bonded complex between CH_3COOCH_3 and HO^- to TS1a. [e] The energy barrier calculated in gas phase is 3.5 kcal/mol which is the energy change from a hydrogen-bonded complex between $HCOOCH_3$ and HO^- to TS1b.

Table 2. Energy Barriers (in kcal/mol) Calculated by Employing the Hybrid Supermolecule-Polarizable Continuum Approach for the Base-Catalyzed Hydrolysis of Methyl Esters in Aqueous Solution Compared with Experimental Activation Energy[a]

	methyl acetate hydrolysis			methyl formate hydrolysis		
energy calculations on supermolecues	first step	second step[e]	total	first step	second step[f]	total
MP2/6-31++G(d,p)	9.4	9.0	9.4	8.8	7.5	8.8
	[−11.1]	[6.6]		[−11.1]	[6.4]	
MP2/6-311++G(d,p)	10.7	8.8	10.7	10.1	7.4	10.1
	[−9.7]	[6.4]		[−9.8]	[6.4]	
MP2/6-311++G(2d,2p)	11.5	8.4	11.5	10.4	6.7	10.4
	[−9.0]	[6.1]		[−9.5]	[5.6]	
MP2/6-311++G(3d,2p)	11.6	8.1	11.6	10.7^g	6.5	10.7^g
	[−8.9]	[5.8]		[−9.2]	[5.5]	
exptl (in pure water)			10.45^b			9.81^c
exptl (62% acetone in water)			12.2^d			

[a] All calculations used the supermolecular geometries optimized at the B3LYP/6-31++G(d,p) level. The energy barrier in solution is taken as the sum of the energy barrier determined by the MP2 calculations on the supermolecules (including the ZPVE correction) and the corresponding solvent shift determined by the FPCM calculations on the supermolecules at the HF/6-31++G(d,p) level. The values in brackets are the energy barriers determined by the pure supermolecule calculations ignoring the remaining bulk solvent effects. [b] Experimental activation energy from ref 22. [c] Experimental enthalpy of activation from ref 34. [d] Experimental activation energy from ref 23. [e] Results for the pathway involving water-assisted proton-transfer associated with the transition state $TS2a(H_2O)_4$. The results (in kcal/mol) associated with the transition state $TS2'a(H_2O)_4$: 13.9 [11.0]−MP2/6-31++G(d,p); 13.6 [10.7]−MP2/6-311++G(2d,2p); 13.7 [10.8]−MP2/6-311++G(3d,2p). [f] Results for the pathway involving water-assisted proton-transfer associated with transition state $TS2b(H_2O)_4$. [g] The corresponding enthalpy of activation determined by including the thermal correction to enthalpy instead of the ZPVE correction to energy is 10.6 kcal/mol.

The energy barriers listed in Table 1 indicate that the solvent shifts determined by the FPCM calculations at the HF/6-31++G(d,p) level are very close to the corresponding solvent shifts determined by the FPCM calculations at the MP2/6-31++G(d,p) level. The largest difference between the two kinds of results is 0.2 kcal/mol. Thus, the HF/6-31++G(d,p) quantum chemical approximation level is adequate for the FPCM calculations in this study.

As seen in Table 1, the energy barriers calculated for the second step are always significantly higher than those for the first step, which is inconsistent with the conclusion of heavy-atom kinetic isotope studies.[4−6,8] The observed kinetic isotope effects indicate that the first step, i.e. the formation of the tetrahedral intermediate (INT), is rate-determining. With the experimental conclusion in mind, one can see that the pure SCRF calculations significantly underestimate the solvent shift of the energy barrier for the first step because the calculated energy barrier, 7.2 kcal/mol, is significantly smaller than the experimental activation energy, 10.45 kcal/mol[22] (pure water) or 12.2 kcal/mol[23] (62% acetone in water), reported for hydrolysis of methyl acetate.

Energy Calculations on Supermolecules. Let us first discuss the results calculated for the reaction pathway involving a water-assisted proton transfer. The energy barriers calculated with various basis sets are listed in Table 2. Compared to the results calculated for the gas-phase hydrolysis of methyl acetate, the energy barriers calculated for the supermolecular reaction system are more sensitive to the basis set. The energy change from the separated reactants to TS1a was calculated with the 6-31++G-(d,p) basis set as −14.6 kcal/mol, which differs from the result calculated with the 6-311++G(2d,2p) basis set by ∼0.1 kcal/mol. For the supermolecular reaction system, the differences between the energy barriers calculated with the 6-31++G(d,p) basis set and those with the 6-311++G(2d,2p) basis set, about ∼0.6−2.1 kcal/mol, are much larger, especially for the first step of the hydrolysis. Nevertheless, the differences between the results with the 6-311++G(2d,2p) basis set and those with the 6-311++G(3d,2p) basis set are only ∼0.1−0.3 kcal/mol. These results are not surprising, because the basis set superposition errors (BSSE) for the MP2 calculations on the hydrogen-bonded supermolecules are expected to be significantly larger than those for the same level of calculations on the corresponding systems in which the four solvent water molecules are removed. This is why we employed the larger basis sets, in addition to the 6-31++G(d,p), to carry out the MP2 calculations on the supermolecules, even if we had known that the 6-31++G(d,p) basis set is adequate for the calculations on the gas-phase hydrolysis.

Comparing the results listed in Tables 1 and 2, one notes that the extremely large solvent shifts of the energy barriers for the first step of the hydrolysis of the methyl esters are attributed mainly to the contributions of the bulk solvent effects. However, the effects of the hydrogen bonding with solvent water molecules on the energy barriers are also significant. Without explicit consideration of the hydrogen-bonding effects, the calculated energy barriers for the first step of the hydrolysis (based on the pure SCRF calculations) become ∼4−5 kcal/mol smaller.

Concerning the relative magnitudes of the energy barriers for the first and second steps, the results calculated with the different basis sets are qualitatively consistent. For both esters, the energy barriers calculated for the second step involving the water-assisted proton transfer are always lower than those for the first step of the hydrolysis in aqueous solution. According to the results calculated with the 6-311++G(3d,2p) basis set, the barriers for the first step are ~4 and ~5 kcal/mol higher than the barriers for the second step for methyl acetate and methyl formate, respectively. So, the first step should be rate-determining for both esters. This conclusion is qualitatively consistent with the reported experiments.[8h] Quantitatively, the energy barrier for the first step calculated with the 6-311++G(3d,2p) basis set, 11.6 kcal/mol, is in excellent agreement with the reported experimental activation energies, 10.45 kcal/mol[22] (pure water) and 12.2 kcal/mol[23] (62% acetone in water), for the hydrolysis of methyl acetate in the aqueous solution. The energy barrier, 10.7 kcal/mol, and the enthalpy of activation, 10.6 kcal/mol, calculated for the methyl formate hydrolysis in water with the 6-311++G(3d,2p) basis set are also very close to the reported experimental enthalpy of activation, 9.81 kcal/mol[34] (pure water).

The role of the water molecule assisting the proton transfer in the second step of the hydrolysis can be seen from the relative magnitudes of the calculated energy barriers associated with the transition states TS2a(H$_2$O)$_4$ and TS2′a(H$_2$O)$_4$. The energy barrier calculated with the 6-311++G(3d,2p) basis set for the second step associated with TS2′a(H$_2$O)$_4$ is 13.7 kcal/mol, which is 5.6 kcal/mol higher than the barrier, 8.1 kcal/mol, calculated at the same level of theory for the second step of the hydrolysis of methyl acetate associated with TS2a(H$_2$O)$_4$. It follows that the direct participation of the solvent water molecule in the proton-transfer process significantly drops the energy barrier by ~5.6 kcal/mol. This is why the energy barrier for the second step of the hydrolysis involving the water-assisted proton transfer is lower than that for the first step, while the energy barrier for the second step involving the direct proton transfer is higher than that for the first step. Thus, the reaction pathway involving the water-assisted proton transfer should dominate the hydrolysis in aqueous solution.

Now, let us discuss some theoretical issues of the hybrid supermolecule-polarizable continuum approach employed in this study. First of all, it should be pointed out that the hybrid supermolecule-polarizable continuum approach employed in this study is quite different from that used by Florián and Warshel in studying phosphate ester hydrolysis.[35] Their quantum chemical calculations were coupled with the Langevin dipoles (LD) or the PCM calculations, but they did not explicitly include solvent water molecule in their quantum chemical calculations. The hybrid supermolecule-polarizable continuum approach employed in this study is also different from that used by Haeffner et al. to study the methyl acetate hydrolysis.[24] Besides using the different SCRF procedure, two water molecules were explicitly included in their calculations on the second step, while no water molecule was explicitly included in their calculations on the first step. All of the reaction steps were examined at a consistent level of theory in the present study, because four solvent water molecules were explicitly included in our calculations on the whole hydrolysis process. The consideration of the explicit solvent in the first solvation shell was recently discussed by Cramer and Truhlar.[26c] They expressed some concerns about the determination of the number and orientation of the nonbulk

water molecules, because for a complete first solvation shell of a solute there might be a very large number of orientations associated with local minima. However, the supermolecular reaction system studied in this study should be less affected by the orientation problem due to several reasons. First, since the four solvent water molecules all strongly hydrogen-bond to the solutes, the orientation of the supermolecule is simply determined by the solute−solvent hydrogen-bonding pattern examined. Second, the orientations of the four water molecules surrounding reactants, transition states, and intermediates are closely connected with each other because the expected connections were confirmed by the IRC calculations. For example, the solute−solvent hydrogen-bonding pattern of TS1a(H$_2$O)$_4$ determines the solute−solvent hydrogen-bonding pattern of the reactants. Finally, the solute−solvent hydrogen-bonding pattern of the reactants examined in this study might be reasonable for our purpose. The three water molecules extremely strongly hydrogen-bond to hydroxide oxygen. We tried to have four water molecules hydrogen-bonded to hydroxide oxygen without success. It seems that hydroxide oxygen can, at most, have hydrogen bonds simultaneously with three water molecules. The fourth water molecule was chosen to hydrogen-bond to the carbonyl oxygen, instead of the ester oxygen, because the hydrogen bond between water and the carbonyl oxygen should be stronger. Concerning the number of the nonbulk solvent water molecules included in the quantum chemical calculation, only four water molecules were explicitly considered in the present study. It is expected that the results calculated with more nonbulk solvent water molecules could be improved further. However, the explicit consideration of additional solvent water molecules should be less important than that of the first four water molecules, because the solute−solvent hydrogen bonds involving additional water molecules should be weaker than what we have already considered for the four water molecules. Without consideration of any limitation of the available computer resources, the explicit consideration of all of the possible solute−solvent hydrogen bonds in the hydrolysis system would need, at least, five additional water molecules. This is because the possible maximum number of covalent and hydrogen bonds for each oxygen atom may be four. Thus, in the reactants the carbonyl oxygen could simultaneously hydrogen-bond to three water molecules, and the ester oxygen could simultaneously hydrogen-bond to two water molecules. Besides, the hydroxide hydrogen could also hydrogen-bond to a water molecule. The reaction pathway calculation starting from the supermolecular reactants including at least nine solvent water molecules might lead to a second transition state structure in which the ester oxygen has hydrogen bonds with three water molecules. However, it is not likely that all of the nine water molecules could directly hydrogen-bond to the tetrahedral intermediate between the first and second transition states. Two of the nine water molecules might just hydrogen-bond to the remaining water molecules in the intermediate.

Conclusions

We have carried out a series of first-principle calculations by using a hybrid supermolecule-polarizable continuum approach to study the reaction pathways and solvent effects on the energy barriers for the base-catalyzed hydrolysis of two representative alkyl esters in aqueous solution. In the hybrid supermolecule-polarizable continuum approach, four solvent water molecules were explicitly included in the supermolecular reaction coordinate calculations, and the remainder of solvent water was modeled as a polarizable dielectric continuum

(34) Humphreys, H. M.; Hammett, L. P. *J. Am. Chem. Soc.* **1956**, *78*, 521.

(35) Florián, J.; Warshel, A. *J. Phys. Chem. B* **1998**, *102*, 719.

Hydrolysis of Carboxylic Acid Esters in Water

J. Am. Chem. Soc., Vol. 122, No. 11, 2000 2627

medium surrounding the supermolecular reaction system. We have found two competing reaction pathways sharing a common first step, i.e. the formation of the tetrahedral intermediate, for the supermolecular reaction system. One pathway involves a direct proton transfer in the second step, i.e. the decomposition of the tetrahedral intermediate. According to this route of hydrolysis, the energy barrier calculated for the decomposition of the tetrahedral intermediate is always higher than the formation of the tetrahedral intermediate. Another pathway involves a water-assisted proton transfer during the decomposition of the tetrahedral intermediate. The direct participation of the solvent water molecule in the proton-transfer process significantly decreases the energy barrier for the second step of the hydrolysis of methyl acetate by about 5.6 kcal/mol. Thus, the energy barrier calculated for the decomposition of the tetrahedral intermediate through the water-assisted proton-transfer becomes lower than the barrier for the formation of the tetrahedral intermediate.

The favorable pathway involving the water-assisted proton transfer is consistent with the heavy-atom kinetic isotope studies, i.e. that the formation of the tetrahedral intermediate is rate-determining for the ester hydrolysis in aqueous solution. Calculated numerical results also indicate that the extremely large solvent shifts of the energy barriers for the formation of the tetrahedral intermediate are attributed mainly to the contributions of the bulk solvent effects. However, the effects of the hydrogen bonding with solvent water molecules on the energy barriers are also significant. Without explicit consideration of the hydrogen-bonding effects, the calculated energy barriers for the first step of the hydrolysis (based on the pure SCRF calculations) become ~4−5 kcal/mol smaller. The results calculated by using the hybrid supermolecule-polarizable continuum approach including both the hydrogen-bonding effects and the remaining bulk solvent effects are consistent with available experimental results. The energy barriers calculated for the first step of the hydrolysis in aqueous solution are in excellent agreement with the experimental data reported for methyl acetate and methyl formate.

Supporting Information Available: Figures showing the optimized geometries of the transition states, intermediate, and reactant for the hydrolysis of methyl formate and figures showing the optimized geometries of the transition states, intermediate, and reactants for the hydrolysis of methyl acetate indicated with more geometric parameters (PDF). This material is available free of charge via the Internet at http://pubs.acs.org.

JA9937932